Data Analysis for Lightning Electromagnetics

Darwin Goei, Department of Electrical and Computer Engineering
Advisor: Steven A. Cummer, Assistant Professor

Abstract

Two projects were conducted in my independent study. My first project is "Identifying the –CGs with High Charge Moment Changes in U.S.", and my second project is "Relations of Magnetic Field Amplitude and Peak Current in Lightning Strokes".

In the first project, I calculated the charge moment changes in more than 300 cloud-to-ground (CG) return strokes detected by the National Lightning Detection Network (NLDN) in U.S. Peak currents and charge moment changes of the big negative CG strokes (–CGs) extracted do not obey any specific relation. It does not agree with an earlier research result which showed a linear relationship between peak currents and charge moment changes for less powerful "normal" –CGs. Analysis shows that most of the –CGs with high charge moment changes occurred over the Gulf of Mexico and Florida.

In the second project, I extracted several lightning parameters, including time, location, peak current, and recorded magnetic field maximum, for more 200 –CGs detected by the NLDN. Distances between these lightning events and the Duke University ELF magnetic field sensor were calculated. From the plots of recorded B-field maximum vs. peak current and recorded B-field maximum vs. distance, I found that the recorded B-field maximum varies linearly against peak current and exponentially against distance. I also determined the constant terms in the linear and exponential equations and developed a single equation which relates peak current to recorded B-field maximum and distance.

Identifying the –CGs with High Charge Moment Changes in U.S.

1. Introduction

Lightning stroke with high charge moment change is believed to be the cause of electrical breakdown in the upper atmosphere above thunderstorms that creates spectacular optical emissions called sprites [*Neubert*, 2003](see Figure 1). However, almost all of the sprite events that have been spotted occurred in the Midwest and were related to only +CGs. This is very unusual because, in theory, +CGs and –CGs

with high enough charge moment changes are equally likely to produce sprites [*Pasko et al*., 2000]; and globally, high charge transfer -CGs are approximately as abundant as high charge transfer +CGs [*Huang et al.,* 1999]. We suspect that sprite events related to –CGs are occurring somewhere other than the Midwest. To prove this, we first need to identify the –CGs with high charge moment changes and find out where they are located. Then, high-altitude cameras should be set up in those areas to look for –CGs-induced sprites.

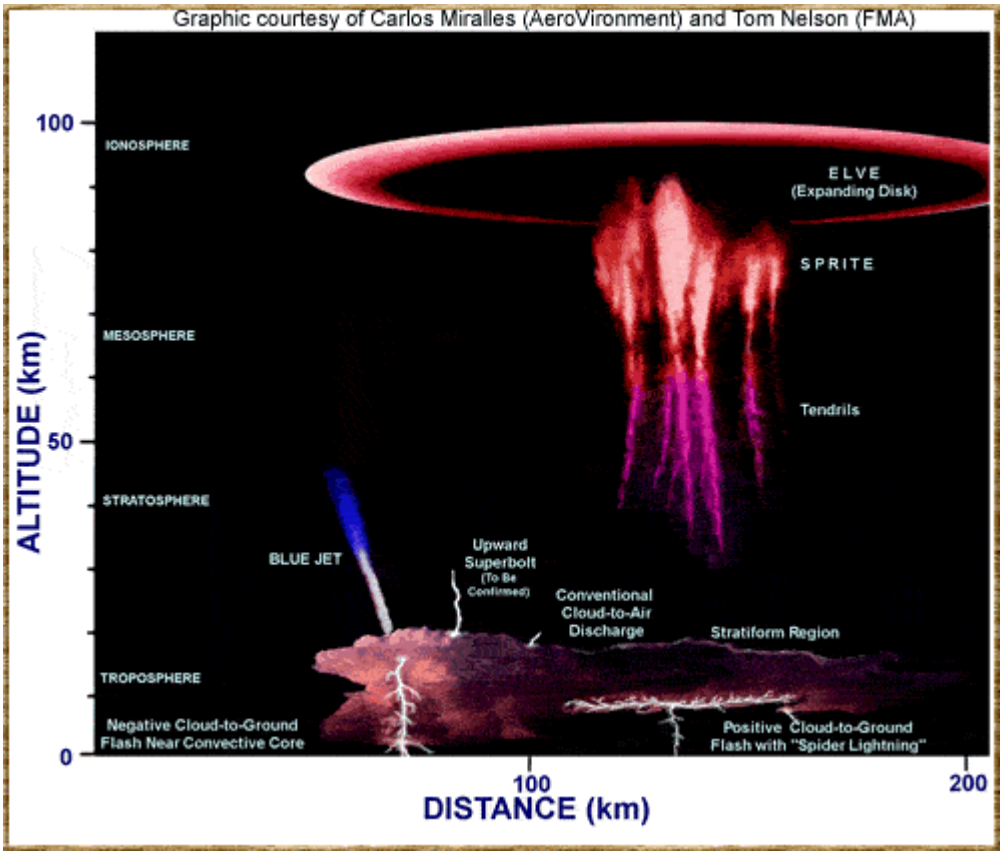

Figure 1. Sprite and other mesospheric optical emissions

2. Instruments, Data, and Analysis Techniques

Some information about lightning, such as its current moment and charge moment change (ΔM_q), is not recorded by the NLDN. ELF (extremely low frequency, ~10—1500Hz) lightning remote sensing [*Cummer and Inan*, 2000] has enabled monitoring of current moment and charge moment change over large geographical areas. We set up a sensor at a field site (35.975°N, –79.100°E) to record the ELF magnetic field waveforms from lightning. The sensor is equipped with GPS absolute timing so that we could unambiguously identify the ELF waveform radiated by every NLDN-detected stroke identified for analysis.

From earlier research, I found that the relationship between charge moment

change and peak current for normal –CGs (absolute peak current smaller than 100 kA) is very close to linear. I, therefore, started the search for –CGs with ΔM_q from the set of stroke with high peak currents. The analysis period of 15 days was randomly chosen to be June 16th and June 30th, 2004. From each of the 15 days, I identified the 60 strokes with highest peak current from the NLDN data. Among these 900 strokes, only 423 of them were extracted successfully from our ELF magnetic field waveform database because a triggered recording system was used for that period of time.

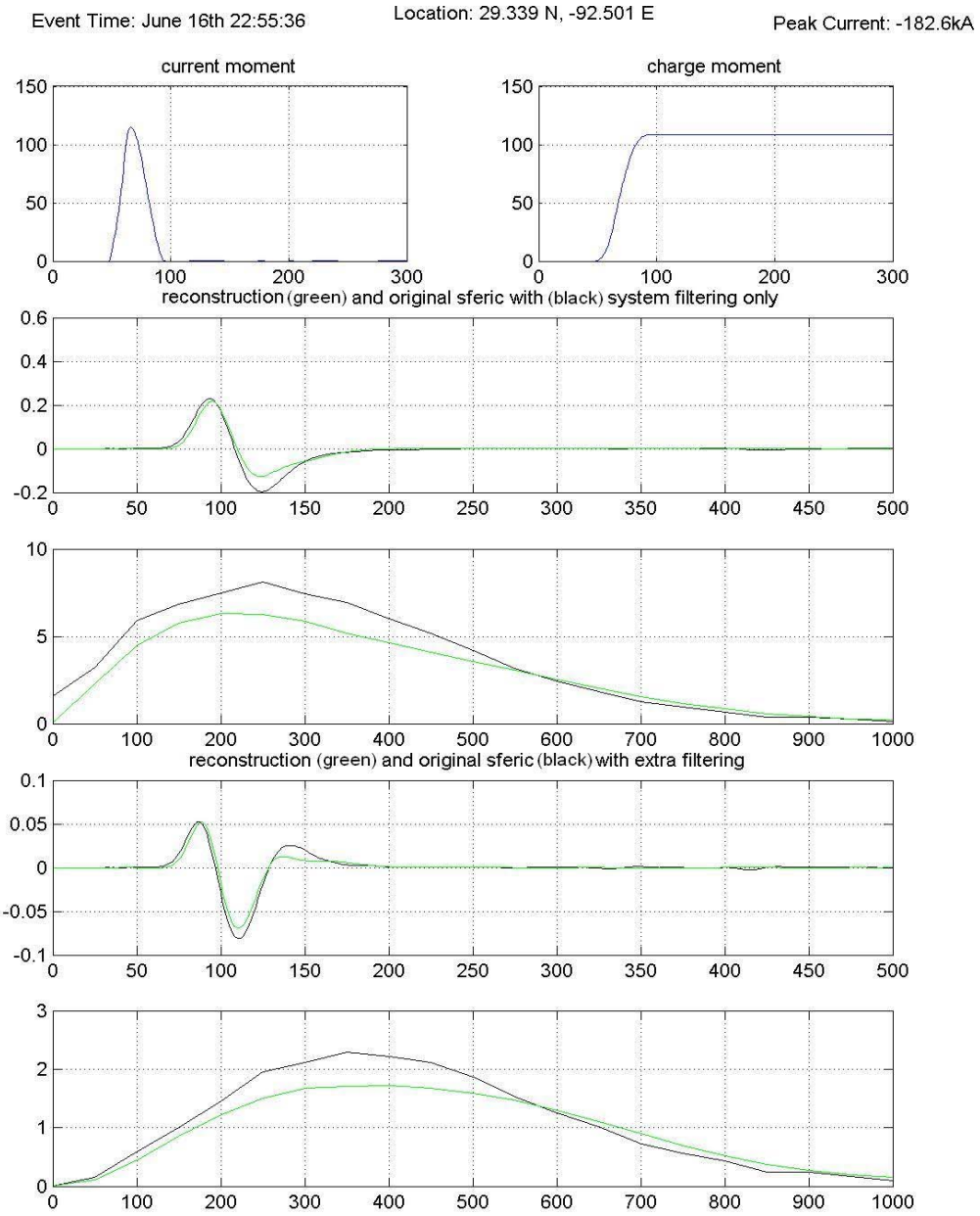

Figure 2. Sample output of deconvolution program

I passed the recorded magnetic field waveforms of these 423 strokes to a

deconvolution program developed earlier using Matlab. The program first estimates the current moment and tries to reconstruct the original waveform by convolving the current moment with an impulse response calculated from several parameters of the stroke. Adjustment is made to the current moment until the difference between the reconstruction and the original waveform is smaller than a threshold. The desired ΔM_q is simply the integration of the final current moment from 0 to 2ms. A sample output of the deconvolution program is shown in Figure 2. After eliminating the events with wrong polarity and excessive noise, ΔM_q of 395 –CGs were obtained. The complete details of the technique used here is described in *Cummer* [2003]

3. Relationship between Peak Current and Charge Moment Change AND Charge Moment Change Distribution

ΔM_q does not relate to peak current in any specific way for –CGs with high peak current, shown in Figure 3. It does not agree with the result of an earlier research which shows a linear relationship between ΔM_q and peak current for normal –CGs. It is very likely that the linear relationship breaks down when the peak current reaches certain threshold and further investigation on such phenomenon should be done. Although I was not able to identify the very biggest –CGs from the set of high-peak-current strokes, this set of strokes gave me a general idea of where the relatively big –CGs are occurring in U.S. as shown in later section.

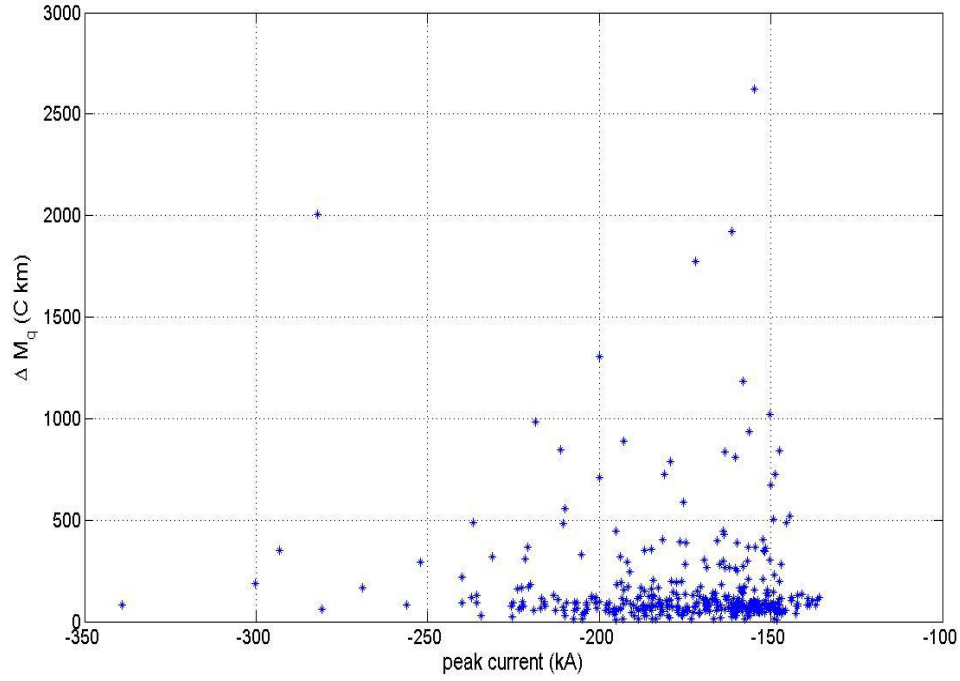

Figure 3. Charge moment change vs. peak current

Figure 4 shows the ΔM_q histogram of –CGs extracted along with their median, mean, and standard deviation. The long tail of the distribution is made into one bar so that the rest of the ΔM_q distribution can be seen clearly. The distribution is smooth and the last bar represents the high- ΔM_q events that we are interested in. Figure 5 is the histogram showing the detail of the long tail.

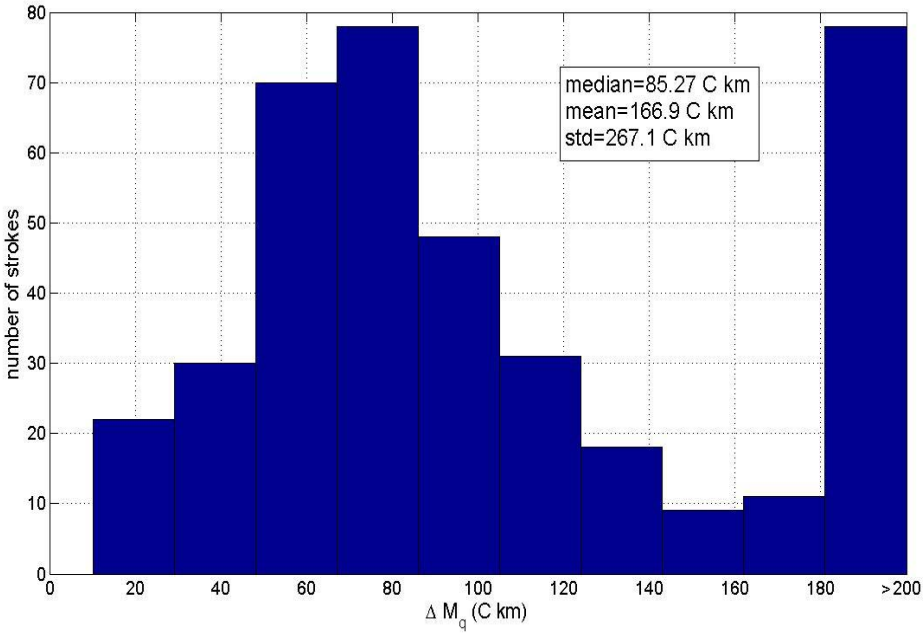

Figure 4. Histogram of charge moment changes

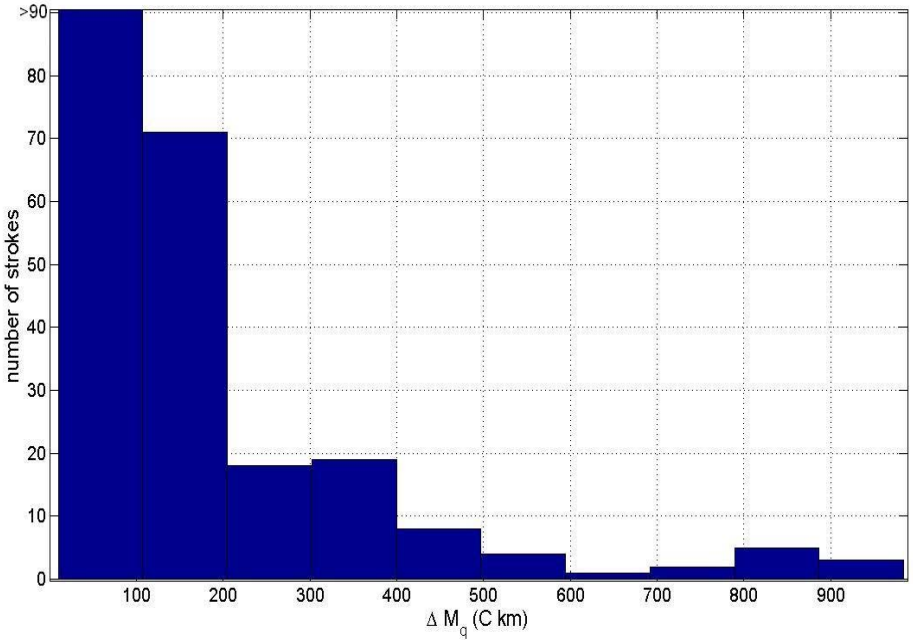

Figure 5. Histogram of charge moment changes showing detail of the long tail

4. Geographical Distribution of –CGs Strokes

We explore the geographical distribution of the >200 C km and <200 C km –CGs extracted. Figure 5 plots the location of the 395 successfully extracted –CG strokes. I plotted the >200 C km strokes with a different symbol (*) than the <200 C km strokes (.) to highlight any differences in the geographical distributions of these two populations. The figure indicates that most of the –CGs occur over the southern part of U.S. while those with ΔM_q>200 C km concentrate over Florida and the Gulf of Mexico.

5. Conclusion

I reported charge moment changes of almost 400 high-peak-current –CG strokes occurring in a 15-day period. The plot of ΔM_q vs. peak current shows that their linear

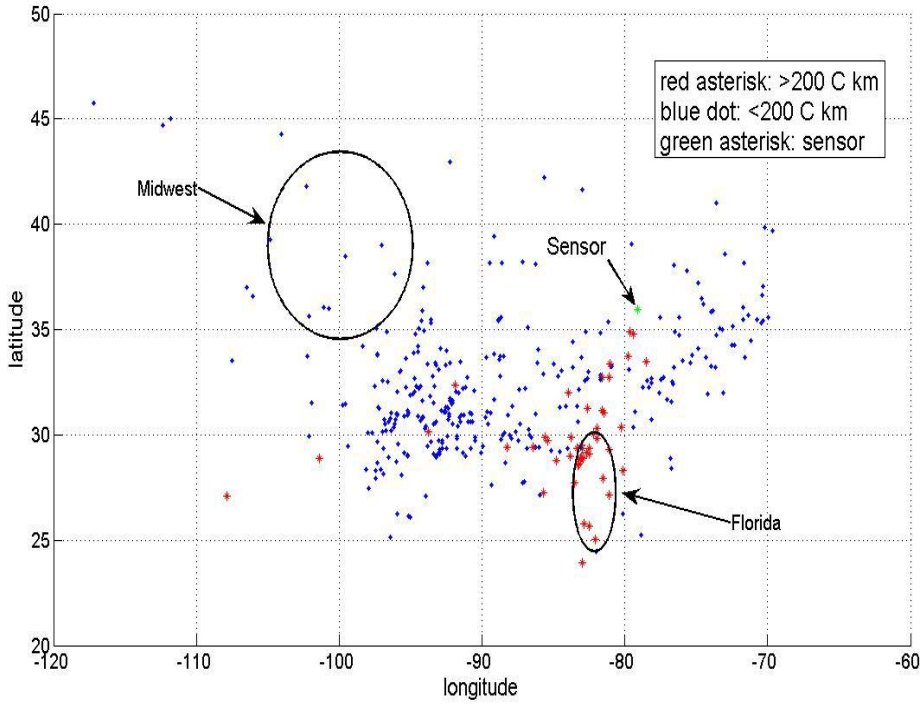

Figure 6. Geographical distribution of >200 C km and <200 C km –CGs

relationship does not hold for strokes with high peak current. Further investigation should be done on determining the limit for the linear relationship to stay true. The ΔM_q distribution is smooth and its long tail represents the possible sprite-inducing lightning events.

The geographical distribution of the –CGs shows that most of the high-ΔM_q –CGs occur over the southeast of U.S. and they are completely absent from the Midwest. This explains why no sprite event related to –CG has been spotted at the

Midwest in the past. In order to make observation for –CGs related sprites, we should draw our attention away from the Midwest and set up several observation spots around Florida.

Relations of Magnetic Field Amplitude and Peak Current in Lightning Strokes

1. Introduction

The NLDN measures only certain lightning parameters, such as time, location and peak current and it has a limited range [*Cummins et al.*, 1998]. Sometimes, we want to independently estimate peak currents from lightning strokes that fall outside the NLDN's range or lightning strokes that were for some reason rejected by the NLDN. Peak radiated field is likely to be closely related to peak current. Therefore, need to extract the peak currents, locations, time, and magnetic field waveforms of lightning strokes from different sources and find out how they are interrelated. After determining all the relationships, we should be able to form an equation relating the peak current to location and magnetic field maximum.

2. Instruments, Data, and Analysis Techniques

There are a lot of factors affecting the relationship between peak current and recorded magnetic field waveform of a lightning event. It is almost impossible to include all these factors into a single equation. Therefore, I restricted my analysis to a specific set of lightning events. The set includes the –CG strokes occurring between 0200 UT and 1000 UT and their distances from our sensor are less than 1200 km and I randomly selected July 10^{th}, 2004 to be the date for data extraction.

NLDN data and ELF magnetic field waveforms of 300 strokes which satisfy the requirements specified above were extracted. The peak currents of the extracted strokes range from -163 kA to -23.9 kA and their distances from our sensor range from 486 km to 1198 km. After eliminating the data with wrong polarity and excessive noise, 286 strokes were used for determining the desired equation.

I first analyzed how recorded magnetic field maximum is related to peak current. To perform the analysis without distance correction, I divided the events into three groups according to their distances from the sensor: <600 km, 600 km-900 km, and >900 km. Curve fitting tool of Matlab was used to determine the best fitting curves of the three groups. The equations of the curves are

<600 km (avg. = 497.8 km): $B = 0.0939 * I – 0.727$ (1)

600 km - <900 km (avg. = 755.9 km): $B = 0.0513 * I – 0.218$ (2)

>900 km (avg. = 1146 km): $B = 0.0403 * I – 0.250$ (3)

The second analysis is on the relationship between recorded magnetic field

maximum and distance from sensor, i.e. distance correction. The events were divided into three groups according to their peak currents: >-50 kA, -50 kA - -80 kA, and <-80 kA. I used the curve fitting tool of Matlab to determine the best fitting curves of the three groups. The equations of the curves are

>-50 kA: B = 3.75 * exp(-0.00105 * D) (4)

-50kA - -80 kA: B = 8.94 * exp(-0.00116 * D) (5)

<-80 kA: B = 9.66 * exp(-0.000852 * D) (6)

The plots for the above two analyses are shown in Figure 6 and Figure 7.

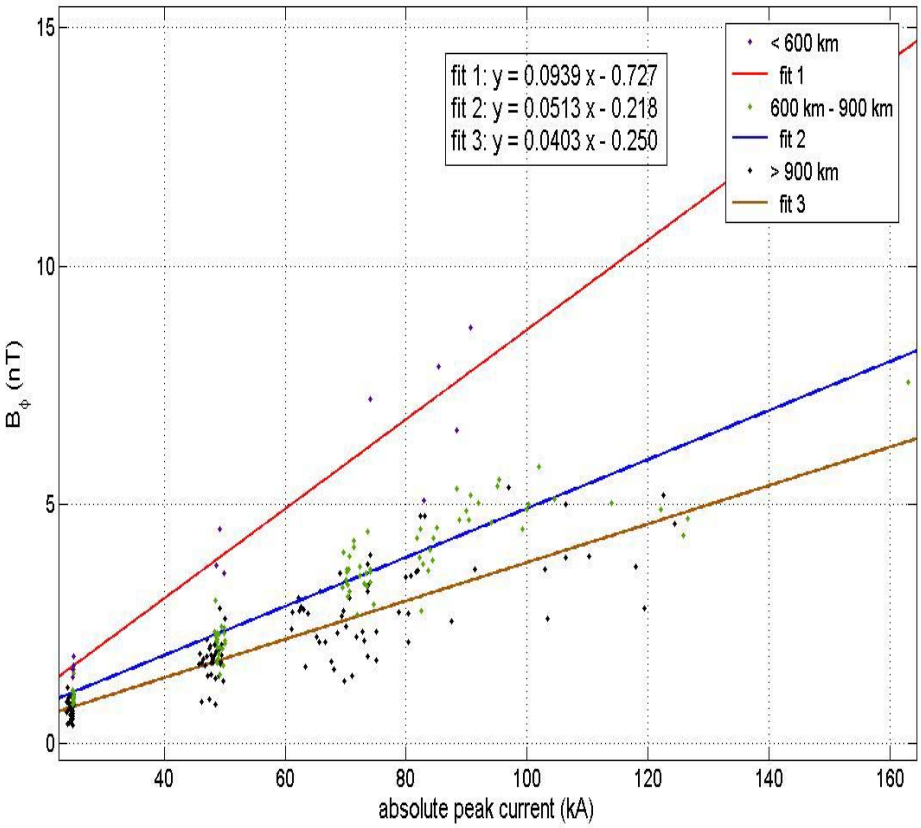

Figure 7. Magnetic field maximum vs. peak current

From the above analyses, I found that the recorded magnetic field maximum varies with absolute peak current linearly and with distance exponentially. Therefore, the final equation relating peak current to recorded magnetic field maximum and distance between event and sensor should be in the following form:

|I| = (B +*c*)/ (*a* * exp(*b* * D), where *a*, *b*, and *c* are constants (*)

Determining constants *b* and *c* is rather easy. To determine *b*, I simply took the average of coefficients of the distance term, D, in equations (4), (5), and (6). The value of *b* turned out to be -0.00102. To determine *c*, the average of the constant terms

in equations (1), (2), and (3) was calculated. I found that the value of *c* was 0.399. It is

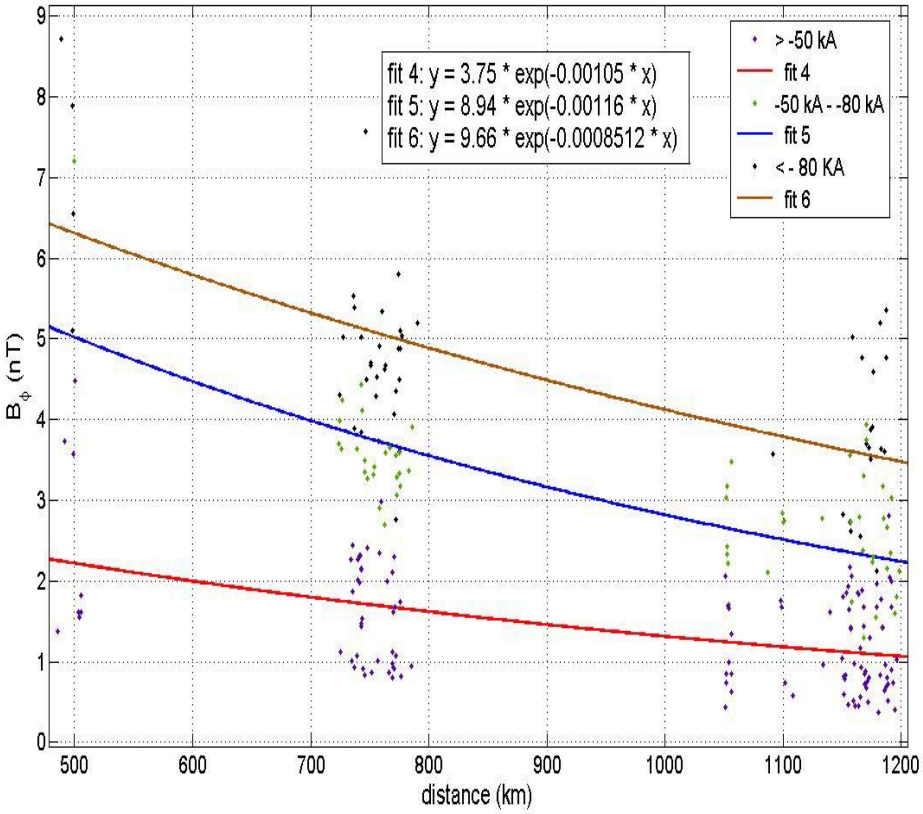

Figure 8. Magnetic field maximum vs. distance

slightly more difficult to determine constant *a*. Since I had already obtained *b*, I was able to apply distance correction to equations (1), (2), and (3). After distance correction, these equations became:

$$B = 0.156 * I - 0.727 \quad (1')$$

$$B = 0.111 * I - 0.218 \quad (2')$$

$$B = 0.130 * I - 0.250 \quad (3')$$

Taking the average of coefficients of the current terms, I found the value of *a* to be 0.132. We now have the values of all three constant terms and the desired equation is:

$$|I| = (B + 0.399) / (0.132 * \exp(-0.00102 * D)$$

3. Error Distribution of Estimated Peak Current

After obtaining the equation, we want to know how close the estimated peak currents are to the NLDN-measured peak currents. I calculated and plotted the absolute error and relative error of the estimated peak currents from the same set of –CG strokes. Absolute error is defined as $|I_{estimated}| - |I_{measured}|$ and relative error is

defined as absolute error/$|I_{measured}|$.

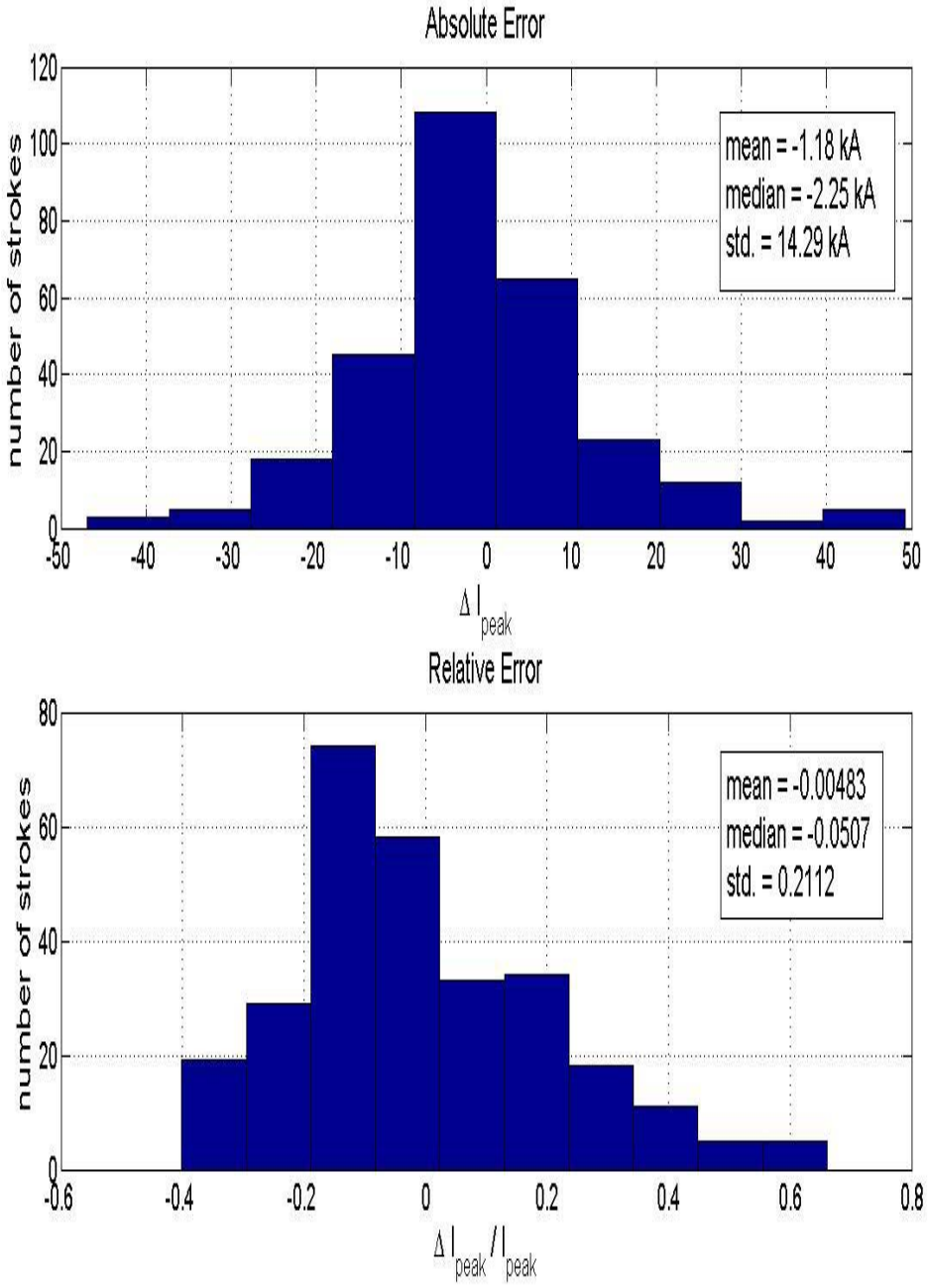

Figure 9. Error Distribution

From Figure 8, we can see that both absolute and relative error distributions are smooth and close to normal. The mean and median of relative error are only -0.00483 (-0.4%) and -0.0507 (-5%) respectively. The estimated peak currents produced by our equation are reasonably close to the NLDN-measured peak currents. This is probably as close as we can get from the measurement.

4. Conclusion

Although the performance of the equation exceeds our expectation, we should note that the equation was only tested by one set of lightning strokes occurred on July 10th, 2004. We will need to test the equation with many other sets of lightning strokes in order to prove its validity. Besides, we can obtain more accurate constant terms *a*, *b*, and *c* in the equation by dividing the strokes into smaller subgroups. It is because we can take the averages over a larger number of terms. Nevertheless, the above approach to obtain equation which relates peak current to recorded magnetic field maximum and distance from sensor was proved to be successful. It should be able to help us answer more questions about lightning and related phenomena.

References

Cummer, S. A. (2003), Current moment in sprite-producing lightning, *J. Atmos. Solar-Terr. Phys., 65,* 499—508.

Cummer, S. A., and U. S. Inan (2000), Modeling ELF radio atmospheric propagation and extracting lightning currents from ELF observations, *Radio Sci., 35*(2), 385—394.

Cummins, K. L., M. J. Murphy, E. A. Bardo, W. L. Hiscox, R. B. Pyle, and A. E. Pifer (1998), A combined TOAMDF technology upgrade of the US National Lightning Detection Network, *J. Geophys. Res.*, 103(D8), 9035—9044.

Huang, E., Williams, E., Boldi, R., Heckman, S., Lyons, W., Taylor, M,, Nelson, T., Wong, C., 1999. Criteria for sprites and elsves based on Schumann resonance observations. *Journal of Geophysical Research 104 (D14),* 16943—16964.

Neubert, T. (2003), On sprites and their exotic kin, *Science, 300*, 747—748.

Pasko, V. P., Inan, U. S., Bell, T. F., 2000. Fractal structure of sprites. *Geophys. Res. Lett. 27 (4*), 497—500.